



**CHALMERS**  
UNIVERSITY OF TECHNOLOGY

## **A case study of the application of AI to early stage drug discovery**

Downloaded from: <https://research.chalmers.se>, 2026-02-28 06:17 UTC

Citation for the original published paper (version of record):

Abdel-Rehim, A., Soldatova, L., King, R. (2026). A case study of the application of AI to early stage drug discovery. *Scientific Reports*, 16(1). <http://dx.doi.org/10.1038/s41598-025-32805-1>

N.B. When citing this work, cite the original published paper.



## OPEN A case study of the application of AI to early stage drug discovery

Abbi Abdel-Rehim<sup>1✉</sup>, Larisa N. Soldatova<sup>2</sup> & Ross D. King<sup>1,3,4,5</sup>

Artificial intelligence (AI) has emerged as a powerful tool in drug discovery, offering the potential to expedite the design of novel therapeutics. This study evaluates the effectiveness of a general-purpose conversational AI, ChatGPT (GPT-4o), in performing three distinct drug discovery tasks, assessing its ability to assist in early-stage molecular ideation and design. In the first task, ChatGPT generated molecules starting from five low-affinity EGFR inhibitors ( $IC_{50}$  values of 10–3.16  $\mu$ M), which were iteratively optimized in a QSAR model to produce compounds with predicted  $IC_{50}$  values of ~10–50 nM. In the second task, de novo design of EGFR inhibitors produced a molecule with a predicted  $IC_{50}$  of 94 nM in a single attempt. In the third task, ChatGPT generated non-covalent MCL1 inhibitors, with a top candidate achieving a docking score corresponding to a 39 nM dissociation constant. Because AI-generated molecules often face synthetic feasibility challenges, we also identified readily available analogues from a chemical vendor. These analogues were evaluated using molecular docking (AutoDock Vina) and QSAR models, with several achieving a promising activity range of 10–100 nM across the three tasks. These results demonstrate that general-purpose AI models like ChatGPT can accelerate early-stage drug discovery by assisting in molecular ideation and candidate prioritization.

Artificial intelligence (AI) has emerged as a powerful tool in drug discovery, with the potential to accelerate the design of therapeutic agents. Traditional processes relying on screening and synthesis are resource-intensive and time-consuming. Recent advances in machine learning, particularly large language models (LLMs), have the potential to streamline early-stage drug discovery by automating molecular design<sup>1–3</sup>.

Most generative AI studies rely on specialized models trained on domain-specific data for tasks such as QSAR modelling, molecular docking, or drug repurposing<sup>4–6</sup>. While models like BioGPT and DrugChat excel within their focused domains, they are often limited to specific tasks and require retraining or integration with other tools for broader applications<sup>7–9</sup>. In contrast, ChatGPT is a general-purpose large language model that is immediately accessible and does not require fine-tuning to begin supporting drug discovery tasks. This versatility makes ChatGPT a flexible and cost-effective solution for researchers without deep AI expertise, particularly in early-stage discovery where rapid ideation and broad exploration are crucial. Instead of relying on multiple specialized models, ChatGPT can generate candidate ideas across several objectives, from hypothesis generation and molecular design to strategic planning, serving as a flexible starting point for researchers<sup>10</sup>.

In this study, we investigate the performance of ChatGPT to support early-stage drug discovery across three *in silico* tasks: QSAR guided design of molecules targeting EGFR, de novo inhibitor design for EGFR, and non-covalent inhibitor design for MCL1 (Fig. 1). Despite existing therapies, both proteins remain active areas of research due to issues like resistance mutations in EGFR (e.g., T790M, C797S) and toxicity or resistance mechanisms in MCL1 inhibition<sup>11–15</sup>. Their extensive structural and functional characterization provides a rich foundation for computational design, making them ideal test cases for evaluating LLM-driven drug discovery.

The goal of this work is not to replace existing workflows, but to assess how a versatile “off the shelf” AI can spark creative hypotheses and propose viable drug candidates before substantial resources are committed. To ensure practical feasibility, we paired ChatGPT’s molecule suggestions with similarity searches in MolPort to identify commercially available analogues suitable for expedient experimental testing.

The first task involved using ChatGPT to design molecules for EGFR from a starting point of five low-affinity compounds ( $IC_{50}$  values of 10–3.16  $\mu$ M), without providing any information about the target protein. After two QSAR-guided iterations, the generated molecules had estimated  $IC_{50}$  values of ~10–50 nM, with corresponding analogues in the range of 20–50 nM, demonstrating successful optimization even without explicit structural context. In the second task, ChatGPT was informed that the target was EGFR and tasked with generating novel EGFR inhibitors in a single attempt, leveraging training-derived associations from its large corpus to propose relevant compounds. Some generated molecules had predicted  $IC_{50}$  values around 100 nM, and the top analogue

<sup>1</sup>Department of Chemical Engineering and Biotechnology, University of Cambridge, Cambridge, UK. <sup>2</sup>Department of Computing, University of London, London, UK. <sup>3</sup>Department of Biology and Biological Engineering, Chalmers University of Technology, Gothenburg, Sweden. <sup>4</sup>Department of Computer Science and Engineering, Chalmers University of Technology, Gothenburg, Sweden. <sup>5</sup>The Alan Turing Institute, London, UK. ✉email: aar52@cam.ac.uk

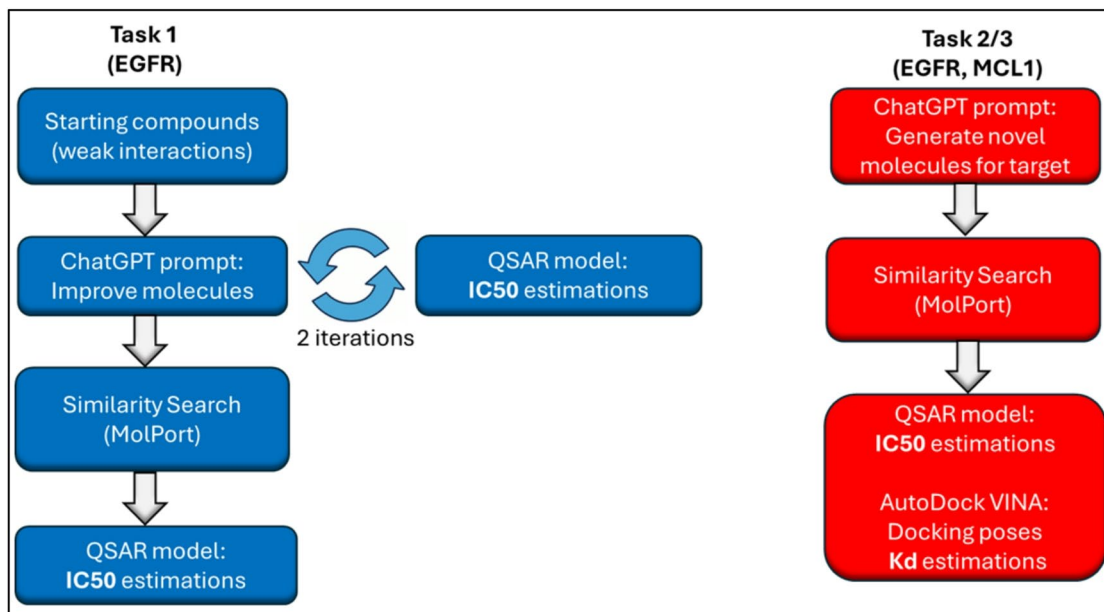


**Fig. 1.** Flowchart describing the two different approaches used in this study. Task 1) Investigate the ability of ChatGPT to generate improved molecules based on weakly binding molecules without mentioning the target (EGFR). Task 2/3) Investigate ChatGPTs ability to generate novel molecules ab initio against two disclosed targets (EGFR, MCL1).

achieved a predicted  $IC_{50}$  value of 56 nM with an estimated dissociation constant of 10 nM. In the third task, focused on MCL1, the top generated molecule achieved a QSAR predicted affinity of 39 nM, though its analogues were not performing as well. The top performing analogue, featuring an added linker, achieved a docking score corresponding to an activity of 108 nM ( $k_d$ ) and a QSAR predicted activity of 46 nM ( $k_i$ ).

These findings demonstrate that output from ChatGPT can support early-stage drug discovery workflows. While not specifically trained for molecular design, ChatGPT generated candidate structures that were used to explore ideation and preliminary optimisation of compounds. As expected, the molecules generated by ChatGPT may not be directly suitable for experimental testing and generally require further *in silico* refinement or analogue-based exploration, as demonstrated in this study. Nonetheless, this work highlights the potential of accessible, general-purpose LLMs to complement traditional approaches and specialized models, particularly when rapid hypothesis generation and broad molecular exploration are needed.

## Materials and methods

### Compound generation and dataset collection

For this study, ChatGPT-4o was used to generate novel molecular candidates for EGFR and MCL1, with the lighter GPT-4o mini model employed in Task 1 to encourage greater creativity. The generated compounds were represented as SMILES strings, and all valid entries were processed for further analysis using RDKit<sup>16</sup>. EGFR ( $IC_{50}$ ) and MCL1 ( $K_i$ ) data was downloaded from ChEMBL. Small molecules were retained for training the QSAR models: <1.1 kDa for EGFR, and the less stringent < 2.5 kDa for the smaller MCL1 dataset.

### QSAR model development and evaluation

$IC_{50}$  and  $K_i$  values for EGFR and MCL1, respectively, were extracted from the ChEMBL database (version 35), and pChEMBL values were calculated as  $-\log_{10}(\text{activity})$  for use in QSAR modeling. Molecular structures were represented as MACCS fingerprints generated from SMILES codes using RDKit (MACCSkeys). For EGFR, a Random Forest model (scikit-learn implementation) with 100 trees and default parameters was trained on the dataset, while the smaller MCL1 dataset (~ 1,000 measurements) was modeled using a Gradient Boosting Regressor with 100 trees and a maximum depth of  $10^{17}$ . Model performance was evaluated using 10-fold cross-validation. For EGFR, the results were Spearman  $R = 0.76 \pm 0.03$ , MSE =  $0.76 \pm 0.09$ , and RMSE =  $0.87 \pm 0.05$ . For MCL1, the corresponding values were Spearman  $R = 0.84 \pm 0.04$ , MSE =  $0.38 \pm 0.04$ , and RMSE =  $0.61 \pm 0.03$ .

### Molecular docking

**Receptor Preparation:** The geometric center of the bound ligand was measured to determine the coordinates for the center of the binding site. The receptor structures (proteins) were obtained from the RCSB Protein Data Bank (PDB code 6FS1 for MCL1 and 3BEL for EGFR). Water molecules were removed, and the protein was saved in PDB format. It was then processed using the prepare\_receptor4.py script from AutoDock Tools to generate a PDBQT file ready for docking.

**Ligand Preparation:** For all tasks, ligands were generated using RDKit. The ligands were processed as follows: hydrogens were added, the molecule was embedded, and MMFF optimization was performed. The final molecules were written to PDB format and converted to PDBQT format using `prepare_ligand4.py` from AutoDock Tools for docking.

**Docking Procedure:** Docking simulations were performed using AutoDock Vina<sup>18,19</sup>. The search space was defined as a cube with dimensions  $20 \times 20 \times 20$  Ångströms, centered around the center coordinates of the binding site. The docking parameters were set to ‘--num\_modes “3”’, ‘--exhaustiveness “20”’ and ‘--energy\_range “7”’ to balance search thoroughness and speed. The resulting binding affinities were reported as estimated  $K_d$  values and used to assess the compounds. Image generation of molecular structures was done in ChimeraX<sup>20</sup>.

### Similarity search

A Chemical Similarity Index was used to perform similarity searches on the MolPort platform<sup>21</sup>. The top 10 or 5 most similar compounds to the selected AI-generated molecules were retrieved, and their predicted binding affinities were evaluated using the same QSAR model.

## Results

### Task 1: drug design for EGFR using iterative procedure

For task 1, three initial batches of compounds were provided to ChatGPT, each containing five structurally diverse molecules with moderate activity values (pChEMBL: 5.01–5.47, corresponding to  $IC_{50}$  values of ~3–10  $\mu$ M). These batches included scaffolds and functional groups common in kinase inhibitors, such as halogenated aromatics, heterocycles, and polar groups like nitriles and hydroxyls. The molecular structures and SMILES codes for these compounds are detailed in Table S1 and S2. This diversity provided a broader chemical space for ChatGPT to explore.

Three independent experiments were conducted to evaluate ChatGPT’s ability to iteratively optimize molecular designs for EGFR using QSAR-guided predictions. The QSAR model used for evaluation was built using available small-molecule  $IC_{50}$  measurements against EGFR in ChEMBL (see methods). Each experiment consisted of two iterations, and the top-predicted molecules after the final iteration (iteration 2) for each batch and experiment are summarized in Table 1 and Table S3 and S4.

The molecular structures of the top predicted compounds from each batch and experiment (9 compounds in total) are shown in Table S3, with corresponding SMILES strings listed in Table S4. These molecules show substantial improvements in predicted binding affinities over the starting compounds.

Notably, the generated molecules showed structural diversity across scaffolds and functional groups, including halogenated aromatics, heterocycles, and polar substituents, contributing to improved binding affinity predictions.

ChatGPT appears to extract key scaffolds from the poorly performing initial molecules. Several generated molecules share features with known EGFR inhibitors, including 4-quinazolineamine and benzimidazole derivatives, as well as halogenated aromatic rings, all of which align with known EGFR inhibitor pharmacophores and indicate that ChatGPT’s generative process reflects established structure-activity relationships<sup>22–25</sup>.

Some molecules feature unconventional elements for EGFR inhibitors, such as a thiourea-containing heterocycle (mol 1.6), a thiophene with multiple substitutions including bromine and a fluoro group (mol 1.7), and a sulfone group (mol 1.9). These atypical structures increase chemical diversity and may enable exploration of novel binding modes or resistant EGFR variants.

This combination of structurally familiar and unusual scaffolds highlights ChatGPT’s ability to leverage known features while proposing novel approaches to molecular design.

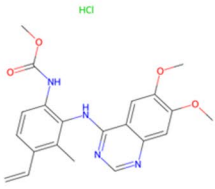
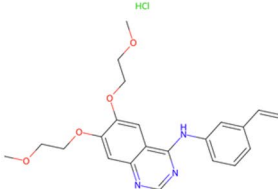
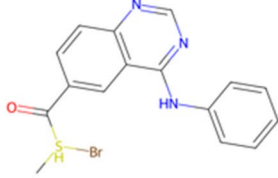
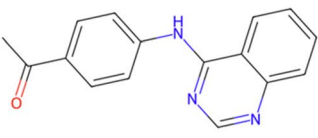
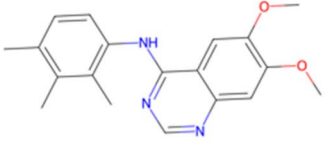
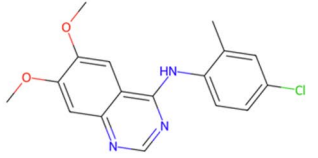
### Similarity search and validation of predicted molecules

A similarity search of the MolPort catalog was performed to assess the practical utility of the GPT-generated molecules (see methods). This search identified commercially available compounds most similar to the highest-affinity predictions from the final QSAR-guided iteration. Top-ranked analogues were evaluated with the QSAR models to confirm strong predicted affinities. Three identified molecules belonged to the class of 4-quinazolineamine derivatives, a well-established scaffold for EGFR inhibition.

All three compounds are experimentally confirmed EGFR binders, supporting the GPT-designed molecules as valid starting points for optimization. The structural similarity between the identified compounds and GPT predictions shows that a general-purpose model can converge on known pharmacologically relevant scaffolds without target-specific training. The structures of these identified 4-quinazolineamine derivatives, along with their respective predicted binding affinities, are shown in Table 2.

	Exp. 1	Exp. 2	Exp. 3
Batch 1	32 nM (7.492)	330 nM (6.481)	52 nM (7.281)
Batch 2	52 nM (7.287)	48 nM (7.315)	24 nM (7.624)
Batch 3	105 nM (6.979)	106 nM (6.947)	11 nM (7.950)

**Table 1.** Predicted activities ( $IC_{50}$  values with corresponding pChEMBL values in brackets), for the top generated molecule from each randomly selected batch of five start molecules, across three independent experiments.

LLM generated query	QSAR (IC <sub>50</sub> )	Top predicted Molport analogue	Similarity Index (position)	QSAR (IC <sub>50</sub> )
MOL 1.2 	52 nM	MOL 1.10 	0.75 (pos.5)	30 nM
MOL 1.9 	24 nM	MOL 1.11 	0.72 (pos.9)	51 nM
MOL 1.8 	11 nM	MOL 1.12 	0.88 (pos.9)	22 nM

**Table 2.** Molecules identified as 4-quinazolineamine-based derivatives derived from similarity searches in molport based on queries of top GPT-designed molecules. All three analogues (MOL 1.10, 1.11 and 1.12) have previously been confirmed to bind EGFR.

### Non-quinazoline derivatives identified via similarity searches

Beyond quinazolineamine derivatives, the MolPort search revealed structurally diverse non-quinazoline compounds resembling the GPT-designed molecules. Four compounds (MOL 1.16–1.19, Table 3) represent opportunities for scaffold hopping in kinase inhibitor development.

Molecules 1.16–1.18 lack prior reports of EGFR inhibition, making them interesting candidates for experimental validation. Molecule 1.19 is linked to a patent for Protein Kinase C (PKC) inhibitors<sup>26</sup>. Since PKC shares an ATP-binding domain with EGFR, cross-reactivity is possible, but kinase-specific differences underscore the need for careful evaluation.

Molecules 1.16–1.18 feature unique structural motifs. Molecule 1.17 originates from a malaria drug discovery library (ChEMBL5016744). Its structural motifs may offer interesting opportunities for kinase inhibition.

In conclusion, ChatGPT generated molecules that improved affinity toward EGFR. Similarity searches demonstrated that these outputs could guide the selection of viable candidates for experimental follow-up, addressing limitations in synthesizability. The system proposed both known scaffolds, such as 4-quinazolineamine derivatives, and novel hinge-binding structures suitable for ATP-competitive kinase inhibition. Compounds such as 1.15–1.17 highlight opportunities for testing, while 1.19 may exhibit cross-kinase activity. Overall, these results illustrate ChatGPT's ability to expand chemical space exploring both familiar and novel scaffolds, supporting early-stage drug discovery.

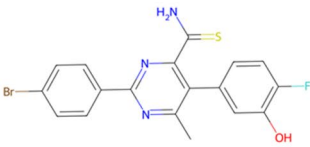
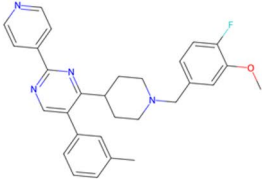
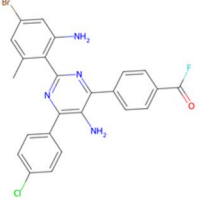
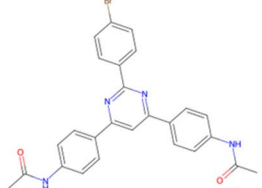
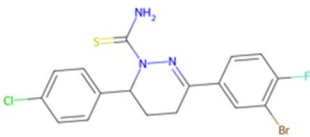
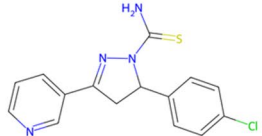
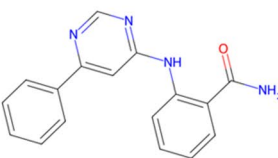
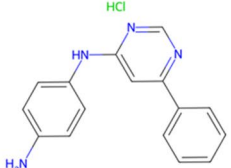
### Task 2: design of novel EGFR inhibitors and identification of potent hits via similarity search

In task 2, ChatGPT, prompted as a drug development expert, designed five novel molecules with strong predicted affinity for EGFR. The aim was to propose structurally distinct starting points emphasizing novelty, drug-likeness, and synthetic feasibility (Appendix A).

For each of the three experiments, the top QSAR predicted molecule had estimated IC<sub>50</sub> values of 94 nM, 116 nM, and 338 nM (Table 4). Their SMILES were used in MolPort to identify the 10 most similar commercially available analogues per molecule, whose predicted binding affinities were also evaluated (Appendix B). The top analogues showed predicted IC<sub>50</sub> values of 55 nM, 56 nM, and 165 nM for each of the three experiments (Table 4), demonstrating that similarity searches can uncover structural diverse compounds with comparable or even improved predicted binding affinities.

Top analogues were then docked using AutoDock Vina to assess EGFR interactions. Docking estimated binding affinities (K<sub>d</sub>) of 1.35 μM, 10 nM, and 77 nM for the leading compounds from each experiment, indicating strong binding affinity (Table 4).

Remarkably, the best-performing molecule, Mol 2.5, corresponds to omilancor, an FDA-approved compound with no reported EGFR activity<sup>27</sup>, achieving an estimated K<sub>d</sub> of 10 nM. Resultant docking poses suggest that its

LLM generated query	QSAR (IC50)	Top predicted Molport analogue	Similarity Index (position)	QSAR (IC50)
MOL 1.13 	87 nM	MOL 1.16 	0.57 (pos.4)	356 nM
MOL 1.1 	32 nM	MOL 1.17 	0.64 (pos.3)	40 nM
MOL 1.14 	113 nM	MOL 1.18 	0.66 (pos.10)	196 nM
MOL 1.15 	54 nM	MOL 1.19 	0.78 (pos.6)	47 nM

**Table 3.** Structures of non-quinazoline-based molecules MOL 1.16–1.19, along with molecules identified through a molport similarity search, the chemical similarity index for the analogues and their rankings amongst the top 10 similar molecules in molport (position), and QSAR predicted activities. SMILES codes for the molecules can be found in Table S4.

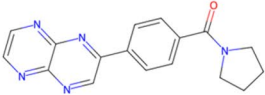
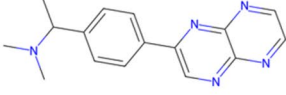
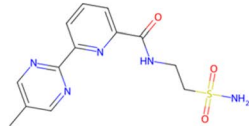
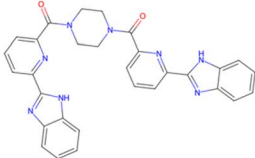
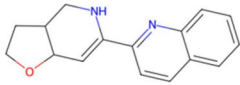
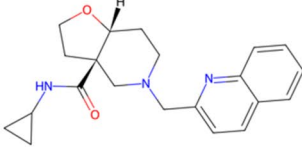
extended conformation reaches deep into the EGFR binding pocket (Fig. 2). The benzimidazole group at one end of the molecule is positioned close to the hydrophobic residues Phe856 and Met766, important contacts in known EGFR inhibitors<sup>28</sup>, while the benzimidazole group on the opposite end bends onto the pocket surface, potentially stabilizing the ligand through hydrophobic interactions. The pyridine may form a potential hydrogen bond with Thr854, a key residue involved in ligand binding. The secondary amine lies close to Asp855 (3.69 Å) and Thr845 (3.28 Å), suggesting additional hydrogen bonding<sup>29</sup>. The central ketone-piperazine-ketone motif bridges hydrophobic and polar regions, providing amphiphilic flexibility. Piperazine has been employed in several EGFR inhibitors to improve solubility and selectivity<sup>30,31</sup>. It is important to note that our docking experiments do not account for explicit water molecules, protein flexibility and solvent effects which could influence binding predictions. Overall Mol 2.5's extended, mirror-like arrangement of benzimidazoles appear to maximize interactions within the pocket, suggesting a favourable fit and a promising candidate for further optimization.

Overall, ChatGPT-generated molecules in task 2, combined with similarity searches, produced structurally diverse, readily accessible candidates with competitive predicted affinities for EGFR inhibition. For an overview of all generated compounds and their predicted activities, as well as the top 10 similar molecules retrieved from MolPort with their similarity scores, see Appendices A and B.

### Task 3: de novo design of non-covalent inhibitors for MCL1

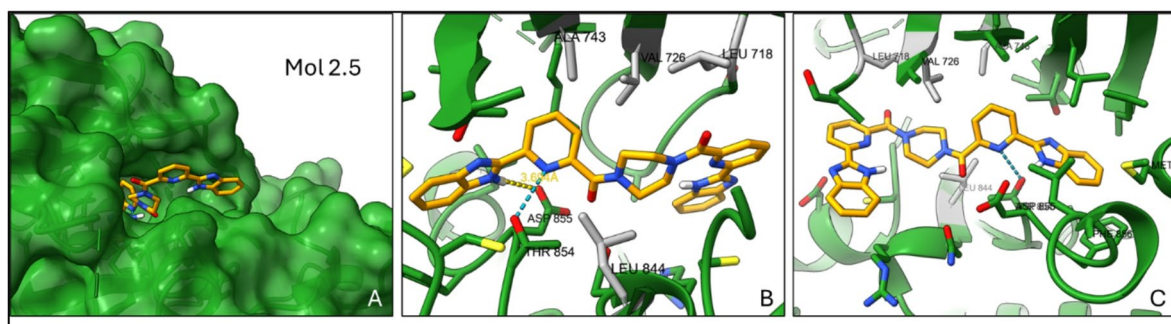
In task 3, ChatGPT was used to design non-covalent inhibitors for MCL1, a BCL2 family protein linked with poor tumor outcomes<sup>32</sup>. Five experiments were conducted, each proposing five molecules. From these experiments, six compounds achieved estimated binding affinities of -9 kcal/mol ( $K_d=250$  nM) or better (Table S6).

Similarity searches against MolPort retrieved the top five most similar compounds for each of the six molecules (Appendix B). Top ranked analogues showed estimated binding affinities of -10.5 to -9.0 kcal/mol ( $K_d\sim 10$  to 250 nM) (Table 5).

Experiment	LLM generated query	QSAR (IC <sub>50</sub> )	Top predicted Molport analogue	Similarity Index (position)	QSAR (IC <sub>50</sub> )	VINA (Kd)
Exp 1	MOL 2.1 	94 nM	MOL 2.4 	0.77 (pos.9)	55 nM	1.35 uM
Exp 2	MOL 2.2 	116 nM	MOL 2.5 	0.6 (pos.5)	56 nM	10 nM
Exp 3	MOL 2.3 	338 nM	MOL 2.6 	0.63 (pos.7)	165 nM	77 nM

**Table 4.** Summary of the top ChatGPT-generated EGFR inhibitor from each of three experiments in task 2, and their QSAR-predicted IC<sub>50</sub> values.

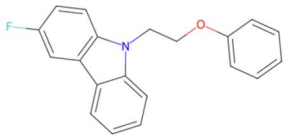
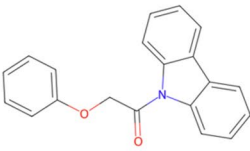
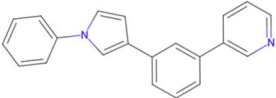
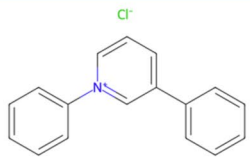
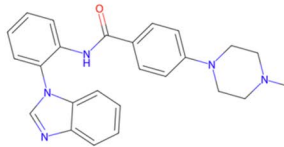
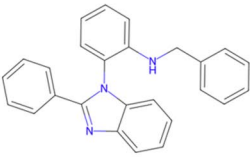
The table also includes the highest-scoring Molport analogues for each compound, their respective chemical similarity index, their rankings amongst the top 10 similar molecules in MolPort (position), along with their QSAR-predicted IC<sub>50</sub> and docking-estimated K<sub>d</sub> values. SMILES codes for molecules can be found in Table S5.



**Fig. 2.** Docking simulation of molecule 2.5 in the EGFR binding pocket (3BEL). (A) Surface representation of the EGFR structure with molecule 2.5 (omilancor) entering the binding pocket. (B) Close-up view of the hydrophobic residues (ALA743, VAL726, LEU718) just past the entrance. Also highlighted are the hydrogen bond with Thr854 (blue dashes) and the estimated distance of 3.694 Å for a potential hydrogen bond with Asp855 (yellow dashes). (C) Full view of the molecule extending deep into the EGFR binding pocket, showcasing its unique conformation and interactions with key residues, including hydrophobic and hydrogen bond interactions.

A QSAR model was built using ~1000 compounds with known K<sub>i</sub> values from ChEMBL. The molecule with the highest estimated docking affinity, Mol 3.6, achieved a modest QSAR prediction of ~1800 nM (K<sub>i</sub>). The top scoring conformation for this docked ligand revealed a quinazoline core positioned near the entrance of the binding pocket, with two hydrophobic benzene rings extending into the highly hydrophobic region of the cavity (Fig. 3). Another hydrophobic benzene ring near the entrance appears to interact with surface hydrophobic residues, likely enhancing the overall fit.

An attempt was made to introduce a functional group capable of forming a hydrogen bond with Arg263, a key residue of the MCL1 binding site, while maintaining a good fit within the hydrophobic pocket. Using ChatGPT, 20 linkers were generated to connect the core structure to functional groups that could facilitate this interaction (Appendix A). Three linkers demonstrated significant improvements in QSAR predictions, with predicted K<sub>i</sub>

Experiment	LLM generated query	VINA (Kd)	Top predicted Molport analogue	Similarity Index (position)	QSAR (IC50)	VINA (Kd)
Exp 1	MOL 3.1 	39 nM	MOL 3.4 	0.78 (pos.4)	1300 nM	20 nM
Exp 2	MOL 3.2 	108 nM	MOL 3.5 	0.77 (pos.1)	7943 nM	210 nM
Exp 3	MOL 3.3 	91 nM	MOL 3.6 	0.68 (pos.3)	1866 nM	12 nM

**Table 5.** Potential candidates for MCL1 binding.

The table presents the top three generated molecules (mol 3.1, 3.2, and 3.3) from three independent experiments along with their estimated affinities ( $K_d$ ) from VINA. The corresponding top hits from the MolPort database (mol 3.4, 3.5, and 3.6) are shown alongside their chemical similarity index, ranking amongst the top 5 similar molecules in MolPort (position), QSAR-predicted activities ( $K_i$ ), and VINA affinity estimations ( $K_d$ ).

values below 100 nM. One linker formed a hydrogen bond with Arg263, stabilizing the complex (Fig. 3C). QSAR predicted the  $K_i$  to improve from  $\sim 1 \mu\text{M}$  to 46 nM, while the docking affinity remained favourable at  $-9.5 \text{ kcal/mol}$  ( $K_d \sim 108 \text{ nM}$ ), providing a reasonable basis for further exploration.

## Discussion and conclusion

This study evaluated ChatGPT, a general-purpose large language model, for generating novel molecular candidates across three drug discovery tasks. Despite not being trained for drug design, the model proposed chemically coherent molecules with competitive predicted affinities and diverse scaffolds. To address practical feasibility, commercially available analogues were identified and evaluated using QSAR modelling and molecular docking, illustrating how accessible AI can support idea generation and candidate prioritization.

While this study used coding to build machine learning models and perform molecular docking, similar analyses can be conducted using user-friendly platforms such as AutoDock for docking, and ChemSAR or OCHEM for QSAR modelling, which require no coding experience<sup>18,19,33,34</sup>. Even without these tools, researchers can evaluate LLM-generated molecules and analogues using rational design principles.

In task 1, starting from low-affinity EGFR inhibitors, two rounds of QSAR-guided design yielded analogues with predicted  $\text{IC}_{50}$  values of 20–50 nM, even when their chemical similarity to the generated molecules was modest (as low as 0.6). In the second task, where EGFR was specified, a top analogue achieved an estimated  $\text{IC}_{50}$  of 56 nM. In the third task, focusing on MCL1, docking of analogues suggested promising estimated activity ( $K_d \sim 10\text{--}200 \text{ nM}$ ), but QSAR predictions for these same molecules exceeded  $1 \mu\text{M}$ . Incorporating linkers proposed by ChatGPT restored predicted potency, with one analogue achieving QSAR affinity of 108 nM and a docking score of  $-9.5 \text{ kcal/mol}$  ( $K_d \sim 108 \text{ nM}$ ).

Across all tasks the model reliably produced chemically coherent structures: in task 1 an average of 42.5 SMILES were generated per run with validity averaging  $\sim 79\%$  across experiments. Tasks 2 and 3 resulted in  $\sim 87\%$  and  $\sim 92\%$  valid molecules respectively. Lipinski's Rule of Five analysis of the featured analogues showed that 2 of 7 task 1 analogues, and 1 of 3 task 2 analogues violated at least one criterion, while all task 3 analogues were fully compliant. Nevertheless, all these candidates were deemed suitable for further exploration as no severe violations or outliers were observed (Table S.7).

Comparison between molecules from tasks 1 and 2 show that both approaches generated promising candidates for EGFR inhibition, though variability between batches and experiments complicates direct ranking. Considering the top three identified analogues, the average predicted activity ( $\text{IC}_{50}$ ) in task 2 was  $7.10 \pm 0.27$ , ranking second relative to the three task 1 batches ( $6.55 \pm 1.29$ ;  $7.61 \pm 0.07$ ;  $6.76 \pm 0.59$ ). Looking beyond averages, two of three task 2 experiments produced analogues with predicted affinities of  $\sim 7.25$  ( $\text{IC}_{50} \sim 56 \text{ nM}$ ), whereas five of nine experiments across all batches in task 1 resulted in molecules with stronger predictions.

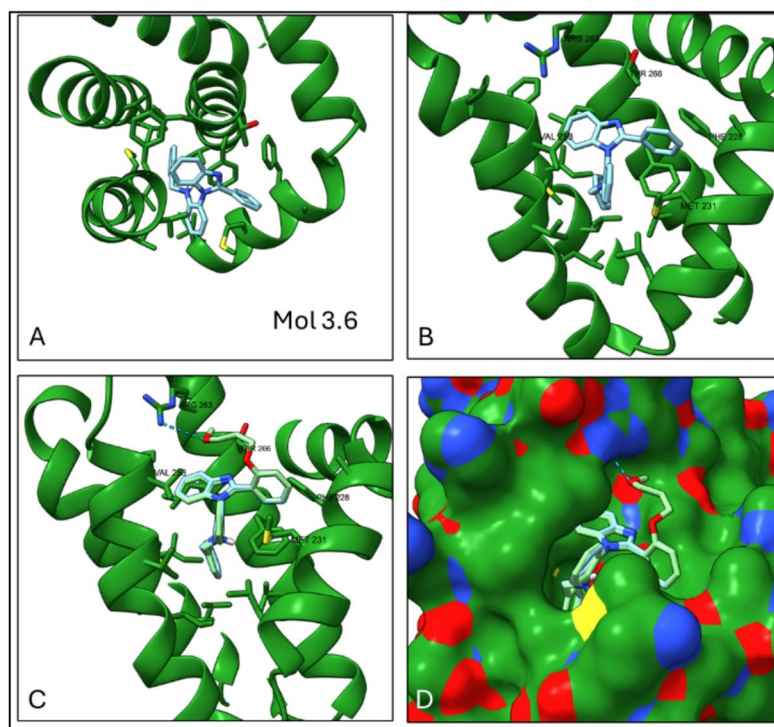


**Fig. 3.** Docking simulation of molecule 3.6 in the MCL1 binding pocket. **(A)** Intercalation of molecule 3.6 with the helices in the MCL1 structure (6FS1). **(B)** The molecule firmly positioned in the hydrophobic pocket, in close proximity to key amino acids MET231 and VAL253. **(C)** Overlap of molecule 3.1 with its linker-modified form (-OCCCO), highlighting a hydrogen bond to ARG263 (blue dashes). **(D)** Surface representation of MCL1 with both the original (blue) and linker-modified (green) molecules superimposed in the binding pocket.

Where molecules were generated *ab initio*, we assessed how much of their architecture reflected known inhibitors versus novel designs. EGFR molecules echoed familiar motifs, particularly nitrogen-rich aromatics, while introducing variation through side-chain designs. Notably, omilancor emerged as an unexpected candidate. MCL1 candidates were generally smaller than well-known inhibitors like Tapotoclax, MI-238, or AZD5991, yet retained recognizable elements, including benzamide and piperazine fragments, alongside more generic ring systems.

A key strength across all tasks was the structural diversity of the identified molecules, spanning multiple scaffolds and functional groups, which broadens the chemical space and supports downstream optimization. Nonetheless, important limitations remain: general-purpose LLMs are not tuned for drug discovery, predicted affinities require experimental validation, and embedded knowledge may lack depth or be outdated.

Future work should integrate LLMs with predictive screening tools, iterative experimental feedback, and specialized databases to improve accuracy and target relevance. Incorporating real-time experimental data could further refine molecular designs and accelerate translation. At the same time, generative AI for molecule design raises ethical and safety concerns, including the risk of “hallucinated” or unsafe structures, inadvertent use of proprietary data, and intellectual property issues. These tools could also be misused to explore toxic or dual-use chemistries, highlighting the need for careful validation, responsible governance, and clear regulatory oversight.

In conclusion, this study demonstrates that accessible, general-purpose LLMs like ChatGPT can support early-stage drug discovery. By rapidly generating and exploring diverse molecular hypotheses, and identifying feasible analogues, this approach offers a practical pathway to democratize and accelerate candidate discovery.

### Data availability

ChEMBL datasets can be downloaded from <https://www.ebi.ac.uk/chembl/>, structures for EGFR (3BEL) and MCL1 (6FS1) are available at <https://www.rcsb.org/>.

### Code availability

Code and processed data are available in the github repository: <https://github.com/abbiAR/AI-in-Early-Stage-Drug-Discovery-and-Ideation>.

Received: 5 October 2025; Accepted: 12 December 2025

Published online: 26 December 2025

## References

- Chakraborty, C., Bhattacharya, M. & Lee, S. S. Artificial intelligence enabled ChatGPT and large Language models in drug target discovery, drug discovery, and development. *Molecular therapy. Nucleic Acids*. **33**, 866–868. <https://doi.org/10.1016/j.omtn.2023.08.009> (2023).
- Lu, J. et al. Large Language models and their applications in drug discovery and development: A primer. *Clin. Transl. Sci.* **18** (4), e70205. <https://doi.org/10.1111/cts.70205> (2025).
- Ramos, M. C., Collison, C. J. & White, A. D. A review of large Language models and autonomous agents in chemistry. *Chem. Sci.* **16** (6), 2514–2572. <https://doi.org/10.1039/d4sc03921a> (2024).
- Kwon, S., Bae, H., Jo, J. & Yoon, S. Comprehensive ensemble in QSAR prediction for drug discovery. *BMC Bioinform.* **20** (1), 521. <https://doi.org/10.1186/s12859-019-3135-4> (2019).
- Koirala, M., Yan, L., Mohamed, Z. & DiPaola, M. AI-Integrated QSAR modeling for enhanced drug discovery: from classical approaches to deep learning and structural insight. *Int. J. Mol. Sci.* **26** (19), 9384. <https://doi.org/10.3390/ijms26199384> (2025).
- Verma, J., Khedkar, V. M. & Coutinho, E. C. 3D-QSAR in drug design—a review. *Curr. Top. Med. Chem.* **10** (1), 95–115. <https://doi.org/10.2174/156802610790232260> (2010).
- Chakraborty, C. et al. AI-enabled Language models (LMs) to large Language models (LLMs) and multimodal large Language models (MLLMs) in drug discovery and development. *J. Adv. Res.* S2090-1232(25)00109-2. <https://doi.org/10.1016/j.jare.2025.02.011> (2025).
- Luo, R. et al. BioGPT: Generative Pre-trained Transformer for Biomedical Text Generation and Mining. arXiv preprint arXiv:2210.10341. (2022).
- Liang, Y., Zhang, R., Zhang, L. & Xie, P. DrugChat: towards enabling ChatGPT-Like capabilities on drug molecule graphs. (2023). arXiv preprint arXiv:2309.03907.
- Abdel-Rehim, A. et al. Scientific hypothesis generation by large Language models: laboratory validation in breast cancer treatment. *J. R. Soc. Interface.* **22** (227), 20240674. <https://doi.org/10.1098/rsif.2024.0674> (2025).
- Yu, H. A. et al. Acquired resistance of EGFR-Mutant lung cancer to a T790M-Specific EGFR inhibitor: emergence of a third mutation (C797S) in the EGFR tyrosine kinase domain. *JAMA Oncol.* **1** (7), 982–984. <https://doi.org/10.1001/jamaoncol.2015.1066> (2015).
- Huang, L. et al. Design, synthesis and biological evaluation of 2H-[1,4]oxazino-[2,3-f]quinazolin derivatives as potential EGFR inhibitors for non-small cell lung cancer. *RSC Med. Chem.* <https://doi.org/10.1039/d4md01016g> (2025). Advance online publication.
- Gao, C. et al. Annual review of EGFR inhibitors in 2024. *Eur. J. Med. Chem.* **292**, 117677. <https://doi.org/10.1016/j.ejmech.2025.117677> (2025).
- Tantawy, S. I., Timofeeva, N., Sarkar, A. & Gandhi, V. Targeting MCL-1 protein to treat cancer: opportunities and challenges. *Front. Oncol.* **13**, 1226289. <https://doi.org/10.3389/fonc.2023.1226289> (2023).
- Deng, H. et al. Discovery of novel Mcl-1 inhibitors with a 3-Substituted-1H-indole-1-yl moiety binding to the P1-P3 pockets to induce apoptosis in acute myeloid leukemia cells. *J. Med. Chem.* **67** (16), 13925–13958. <https://doi.org/10.1021/acs.jmedchem.4c00643> (2024).
- RDKit accessed : Open-source cheminformatics. (2025). <https://www.rdkit.org>.
- Pedregosa, S. C. I. K. I. T. et al. Scikit-learn: machine learning in python. *J. Mach. Learn. Res.* **12**, 2825–2830 (2011).
- Eberhardt, J., Santos-Martins, D., Tillack, A. F. & Forli, S. AutoDock Vina 1.2.0: new Docking Methods, expanded force Field, and python bindings. *J. Chem. Inf. Model.* **61** (8), 3891–3898. <https://doi.org/10.1021/acs.jcim.1c00203> (2021).
- Trott, O. & Olson, A. J. AutoDock vina: improving the speed and accuracy of Docking with a new scoring function, efficient optimization, and multithreading. *J. Comput. Chem.* **31** (2), 455–461. <https://doi.org/10.1002/jcc.21334> (2010).
- Pettersen, E. F. et al. UCSF chimeraX: structure visualization for researchers, educators, and developers. *Protein Science: Publication Protein Soc.* **30** (1), 70–82. <https://doi.org/10.1002/pro.3943> (2021).
- <https://www.molport.com/shop/find-chemicals> (Accessed 2025).
- Şandor, A. et al. Structure-Activity relationship studies based on Quinazoline derivatives as EGFR kinase inhibitors (2017-Present). *Pharmaceuticals (Basel Switzerland)*. **16** (4), 534. <https://doi.org/10.3390/ph16040534> (2023).
- Anwar, S. et al. Deciphering Quinazoline derivatives' interactions with EGFR: a computational quest for advanced cancer therapy through 3D-QSAR, virtual screening, and MD simulations. *Front. Pharmacol.* **15**, 1399372. <https://doi.org/10.3389/fphar.2024.1399372> (2024).
- Bhatia, P. et al. Novel quinazoline-based EGFR kinase inhibitors: A review focussing on SAR and molecular Docking studies (2015–2019). *Eur. J. Med. Chem.* **204**, 112640. <https://doi.org/10.1016/j.ejmech.2020.112640> (2020).
- Li, Y. et al. Discovery of benzimidazole derivatives as novel multi-target EGFR, VEGFR-2 and PDGFR kinase inhibitors. *Bioorg. Med. Chem.* **19** (15), 4529–4535. <https://doi.org/10.1016/j.bmc.2011.06.022> (2011).
- Smith, J. A. & Doe, R. B. Method for treating cancer (U.S. Patent No. US2008242681A1). U.S. Patent and Trademark Office. (2008). <https://patents.google.com/patent/US2008242681A1>.
- Tubau-Juni, N. et al. First-in-class topical therapeutic Omilancor ameliorates disease severity and inflammation through activation of LANCL2 pathway in psoriasis. *Sci. Rep.* **11** (1), 19827. <https://doi.org/10.1038/s41598-021-99349-y> (2021).
- Martorana, A., La Monica, G. & Lauria, A. Quinoline-Based molecules targeting c-Met, EGF, and VEGF receptors and the proteins involved in related carcinogenic pathways. *Molecules (Basel Switzerland)*. **25** (18), 4279. <https://doi.org/10.3390/molecules25184279> (2020).
- Abouzied, A. S. et al. Synthesis, molecular Docking Study, and cytotoxicity evaluation of some novel 1,3,4-Thiadiazole as well as 1,3-Thiazole derivatives bearing a pyridine moiety. *Molecules (Basel Switzerland)*. **27** (19), 6368. <https://doi.org/10.3390/molecule27196368> (2022).
- Li, M. C. et al. Development of Furanopyrimidine-Based orally active Third-Generation EGFR inhibitors for the treatment of Non-Small cell lung cancer. *J. Med. Chem.* **66** (4), 2566–2588. <https://doi.org/10.1021/acs.jmedchem.2c01434> (2023).
- Yun, C. H. et al. Structures of lung cancer-derived EGFR mutants and inhibitor complexes: mechanism of activation and insights into differential inhibitor sensitivity. *Cancer cell.* **11** (3), 217–227. <https://doi.org/10.1016/j.ccr.2006.12.017> (2007).
- Wang, H., Guo, M., Wei, H. & Chen, Y. Targeting MCL-1 in cancer: current status and perspectives. *J. Hematol. Oncol.* **14** (1), 67. <https://doi.org/10.1186/s13045-021-01079-1> (2021).
- Sushko, I. et al. Online chemical modeling environment(OCHEM): web platform for data storage, model development and publishing of chemical information. *J. Comput. Aided Mol. Des.* **25** (6), 533–554. <https://doi.org/10.1007/s10822-011-9440-2> (2011).
- Dong, J. et al. ChemSAR: an online pipelining platform for molecular SAR modeling. *J. Cheminform.* **9** (1), 27. <https://doi.org/10.1186/s13321-017-0215-1> (2017).

## Acknowledgements

We gratefully acknowledge our laboratory colleagues for generating the data and the developers of the software and computational tools.

### Author contributions

A.A. designed the study, analysed the data, and wrote the main manuscript text. R.K. and L.S. supervised the study. All authors reviewed the work and the manuscript.

### Funding

This research was supported by grants from the UK Engineering and Physical Sciences Research Council (EPS-RC) [EP/R022925/2, EP/W004801/1 and EP/X032418/1].

### Declarations

### Competing interests

The authors declare no competing interests.

### Additional information

**Supplementary Information** The online version contains supplementary material available at <https://doi.org/10.1038/s41598-025-32805-1>.

**Correspondence** and requests for materials should be addressed to A.A.-R.

**Reprints and permissions information** is available at [www.nature.com/reprints](http://www.nature.com/reprints).

**Publisher's note** Springer Nature remains neutral with regard to jurisdictional claims in published maps and institutional affiliations.

**Open Access** This article is licensed under a Creative Commons Attribution 4.0 International License, which permits use, sharing, adaptation, distribution and reproduction in any medium or format, as long as you give appropriate credit to the original author(s) and the source, provide a link to the Creative Commons licence, and indicate if changes were made. The images or other third party material in this article are included in the article's Creative Commons licence, unless indicated otherwise in a credit line to the material. If material is not included in the article's Creative Commons licence and your intended use is not permitted by statutory regulation or exceeds the permitted use, you will need to obtain permission directly from the copyright holder. To view a copy of this licence, visit <http://creativecommons.org/licenses/by/4.0/>.

© The Author(s) 2025